J. Non-Equilib. Thermodyn.
2005 · Vol. 30 · pp. 95–111

Crystallization of struvite from metastable region with different types of seed crystal

Md. Imtiaj Ali* and Phil Andrew Schneider
School of Engineering, James Cook University, Townsville QLD-4811, Queensland, Australia

*Corresponding author (Md.Ali@jcu.edu.au)

Abstract

The main feature of this paper was to recognize struvite crystallization in the metastable region of supersaturation. Thermodynamic equilibria of struvite were simulated to identify the minimum struvite solubility limit, thereafter validated by existing thermodynamic modelling packages such as PHREEQC and the derived data from existing struvite solubility curve. Using laser light scattering detection, spontaneous nucleation was identified by the slow increase of pH in a supersaturated solution of struvite. The crystallization experiment, conducted close to the saturation region in metastable zone, initiated struvite growth. The conducted experiment showed that mother crystal (struvite) was more effective as seeds for struvite crystallization.

1. Introduction

The thermodynamically metastable zone is defined as the critical zone of solution supersaturation where crystallization is not governed by nucleation and thus avoids rapid or spontaneous precipitation. Supersaturated solutions induce crystallization by nucleation and subsequent crystal growth. On the basis of the classical theory of crystallization, documented by Gibbs-Thomson, crystallization is a process of energy transformation [1, 2]. Crystal clusters form stochastically, consuming energy from the supersaturated solution. Continuous collision of clusters forms stable nuclei. The growth of stable nuclei is an energy-releasing process [1, 2].

Energy for cluster formation is supplied by a thermodynamic driving force in supersaturated solution. The time lag between the supersaturation of solution and the first appearance of concentration decay is theoretically called induction time [1]. A highly supersaturated solution has a shorter induction time, whereas relatively lower supersaturation is characterized by a longer or even infinite induction time. One disadvantage of infinite induction time is the redissolving of induced crystals in solution due to high-energy consumption from a relatively low driving force. In this circumstance,

J. Non-Equilib. Thermodyn. · 2005 · Vol. 30 · No. 2
 DOI 10.1515/JNETDY.2005.007

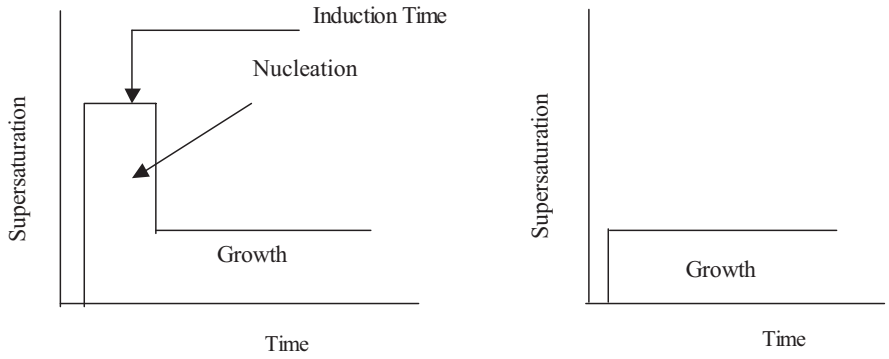

Figure 1 Schematic presentation of crystallization at higher supersaturation and at metastable supersaturation.

preliminary additions of seed materials induce surface diffusion of newly born clusters and govern crystallization [3]. This approach can be obtained when the crystalliser operates along the stable–metastable zone (close to saturation). In industrial crystallization, the metastable zone technique is widely practiced due to smoother continuous operation at controlled supersaturation [4, 5]. A slow decrease of solution supersaturation triggers the addition of reactant into crystalliser. Figure 1 represents the schematic diagram of struvite crystallization at uncontrolled and controlled (stable–metastable) supersaturation.

The metastable zone width is a characteristic property of crystallization, which plays an important role in industrial crystallization to maintain product quality. An attempt at predicting metastable zone width was made by Kim and Mersmann [6] for several organic and inorganic systems in bench-scale cooling crystallization. The approach to determine the metastable zone width of Kim and Mersmann [6] cannot be applied to reactive crystallization since the derived empirical formulation of metastable zone width, relating to different nucleation conditions, is associated with the cooling temperature. The association of thermodynamic driving force/pH value of reactive solution, in the corresponding numerical prediction, is mandatory in reactive crystallization. The model-based prediction of metastable zone width is still in the developing stage; however, the measurement of the metastable zone with the polythermal [6, 7]/poly-thermodynamic driving force [8] under visual or instrumental observation has been documented in the literature. Hirasawa [8] documented an experimental approach of determining metastable zone width for hydroxyapatite, relating to solution supersaturation, pH value, and minimum solubility limit of crystallization. The process described in this paper for the determination of the metastable zone is comprised of a thermodynamic modelling approach along with an experimental approach. Crystallization operated at the metastable zone has the potential for smoother control of systems [9]; however, crystallization occurring at very close to saturation is ultimately a challenging issue [10]. In this respect, seed crystals offer a template of nuclei maturation by providing a diffusive media for newly born thermodynamically unstable nuclei.

The literature suggests that various types of materials are used as seed materials in different types of crystallization. Phosphate rock, bone charcoal, magnesia clinker, zirconium hydroxide, pumice stone, borosilicate glass, struvite, quartz sand, marble, calcium carbonate, activated carbon, bone char, and phosphorus rock, mother crystal (struvite) are the possible candidate seeds [3, 11–15]. Chemical inactivity in the mother liquor, isomorphism with mother crystal, and adequate surface area in suspension are the predominant properties of ideal seeds [1, 2, 16].

2. Mathematical modelling and formulation

Struvite consists of magnesium, ammonium, and phosphate. Solution chemistry plays an important role in struvite formation. In supersaturated solution, struvite forms by the chemical reaction of free Mg^{2+}, NH_4^+, and PO_4^{3-}, as demonstrated in Eq. (1):

$$Mg^{2+} + NH_4^+ + PO_4^{3-} \Leftrightarrow MgNH_4PO_4 \tag{1}$$

The key parameters involved in struvite solution chemistry are solution supersaturation, pH, and the initial concentration of reactants. Solution, consisting of Mg^{2+}, NH_4^+, and PO_4^{3-}, remains in complex forms of Mg^{2+}, $MgOH^+$, $MgH_2PO_4^+$, $MgHPO_4$, H_3PO_4, $H_2PO_4^-$, HPO_4^{2-}, PO_4^{3-}, $MgPO_4^-$, NH_3 (aqueous) [17, 18]. The basic thermodynamic relations of chemical complexes are given in Table 1.

The total constituent concentration for Mg, NH_4, and PO_4, denoting $C_{T,Mg}$, $C_{T,NH4}$, $C_{T,PO4}$, are the total ionic concentration of their complexes and free ions, as illustrated in Eqs. (2–4):

$$C_{T,PO_4} = [H_3PO_4] + \lfloor H_2PO_4^- \rfloor + \lfloor PO_4^{3-} \rfloor + \lfloor MgH_2PO_4^+ \rfloor + [MgHPO_4] + \lfloor MgPO_4^- \rfloor \tag{2}$$

$$C_{T,Mg} = [Mg^{2+}] + [MgOH^+] + \lfloor MgH_2PO_4^+ \rfloor + [MgHPO_4] + \lfloor MgPO_4^- \rfloor \tag{3}$$

$$C_{T,NH_4} = NH_3(aq) + \lfloor NH_4^+ \rfloor \tag{4}$$

Table 1 Thermodynamic equilibria of struvite solution chemistry.

Thermodynamic equations	pK value	References
$\{MgOH^+\} \Leftrightarrow \{Mg^{2+}\} + \{OH^-\}$	$10^{-2.56}$	[19]
$\{NH_4^+\} \Leftrightarrow \{NH_3(aq)\} + \{H^+\}$	$10^{-0.45}$	[20]
$\{HPO_4^{2-}\} \Leftrightarrow \{H^+\} + \{PO_4^{3-}\}$	$10^{-12.35}$	[21]
$\{H_2PO_4^-\} \Leftrightarrow \{H^+\} + \{HPO_4^{2-}\}$	$10^{-7.20}$	[21]
$\{H_3PO_4\} \Leftrightarrow \{H^+\} + \{H_2PO_4^-\}$	$10^{-2.15}$	[20]
$\{MgH_2PO_4^+\} \Leftrightarrow \{Mg^{2+}\} + \{H_2PO_4^-\}$	$10^{-0.45}$	[20]
$\{MgHPO_4\} \Leftrightarrow \{Mg^{2+}\} + \{HPO_4^{2-}\}$	$10^{-2.91}$	[20]
$\{MgPO_4^-\} \Leftrightarrow \{Mg^{2+}\} + \{PO_4^{3-}\}$	$10^{-4.80}$	[20]

Thermodynamic equilibria described above interacts with the pH value of the solution due to the presence of H^+ and OH^-, denoting equilibrium constant of water ($K_w = 10^{-14}$), as shown in Eqs. (5) and (6):

$$[H^+] = 10^{-pH} \tag{5}$$

$$K_w = [H^+][OH^-] \tag{6}$$

The activity coefficient of different components (γ_i) and mean ionic activity coefficient is calculated using the Davies equation (Eqs. [7] and [8]), considering the maximum limit of ionic strength (I) of 0.2 mol/L [22, 23]. The ionisation fraction for Mg^{2+}, NH_4^+, and PO_4^{3-} ($\alpha_{Mg^{2+}}, \alpha_{PO_4^{3-}}, \alpha_{NH_4^+}$) is defined as the quotient of free ion concentration and total concentration of each chemical component,

$$-Log\ \gamma_i = AZ_i^2\left[\frac{I^{1/2}}{1+I^{1/2}}\right] - 0.3I, \tag{7}$$

$$\gamma = (\gamma_{Mg}\gamma_{NH4}\gamma_{PO4})^{1/3}, \tag{8}$$

where

Z_i = valency of the corresponding elements,

A = DeBye-Hückel constant, 0.493, 0.499, 0.509, 0.519 at 5, 15, 25, and 35°C.

Two types of solubility products can express the solubility of struvite crystals, which include conditional solubility product (P_{cs}) and absolute solubility product (P_{so}). The absolute solubility product (P_{so}) relates to solution properties such as ionisation fraction (α_i), activity constant (γ_i), and minimum struvite solubility product (K_{so}), whereas conditional solubility product relates to total concentrations (C_i). Solution of higher conditional solubility product than absolute solubility product ($P_{cs} > P_{so}$) refers to supersaturation. Equal numerical values of P_{cs} and P_{so} characterise the saturated condition, whereas $P_{so} < P_{cs}$ demonstrates undersaturation. The negative logarithmic value of minimum struvite solubility product (pK_{so}) applied in this thermodynamic modelling was 13.26 [18].

$$P_{so} = \frac{K_{so}}{\alpha_{Mg^{2+}}\gamma_{Mg^{2+}}\alpha_{NH_4^+}\gamma_{NH_4^+}\alpha_{PO_4^{3-}}\gamma_{PO_4^{3-}}} \tag{9}$$

$$P_{cs} = C_{T,Mgm}.C_{T,PO4m}.C_{T,NH4m} \tag{10}$$

Solution thermodynamic properties specify the state of saturation, free ion concentrations, type complexes, and state of precipitation/crystallization. The precipitation of struvite occurs in supersaturated solution, which takes place particularly under the influence of the solution's pH value and initial reactant concentration [24]. The dem-

onstrated is based on the magnesium ammonium phosphate precipitation by mixing magnesium chloride and ammonium di-hydrogen phosphate. Presence of base in solution provides increased free ions of phosphate (Eq. [11]), thereby bringing on supersaturation.

$$PO_4^{3-} \Leftrightarrow HPO_4^{2-} \Leftrightarrow H_2PO_4^{-} \Leftrightarrow H_3PO_4 \tag{11}$$

3. Determination of the metastable zone

A series of batch experiments was conducted using a synthetic solution at concentrations of 0.002, 0.003, 0.004, 0.005, and 0.007 molar. Synthetic solution made up of de-ionised water was used in the experiment. Analytical grade $MgCl_2$ and $NH_4H_2PO_4$ were used to make up the synthetic solution, maintaining a molar ratio of $Mg/NH_4/PO_4$ at 1:1:1. The metastable zone experiment was conducted in the absence of seed particles to identify the minimum limit of supersaturation for instantaneous nucleation. The schematic diagram of the experimental set-up is shown in Figure 2. The determination of the metastable zone incorporated two steps, which included (i) the determination of minimum struvite solubility (saturation) by means of the thermodynamic modelling approach and (ii) the determination of minimum saturation limit for instantaneous precipitation by means of the metastable zone experiment approach.

The experiment was conducted in a dark room using a laser light scattering device (laser pointer) for particle detection in which red-colour laser light passed through a reactive solution of 1 L. The reactive solution, contained in 1.5 L of a properly cleaned glass beaker, was agitated using a rotational mechanical agitator with an impeller blade diameter of 2.5 in. A uniform speed of 35 rpm was employed throughout all experiments to provide sufficient mixing of the solution. The solution pH was carefully and slowly adjusted using 0.5 M of NaOH solution at the initial stage and

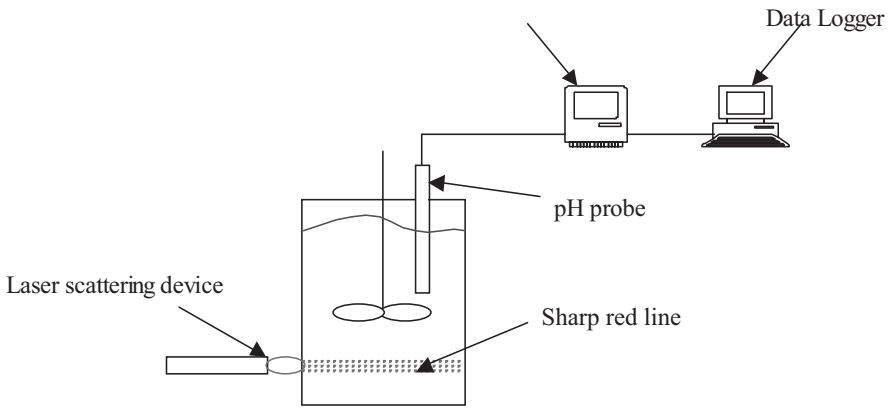

Figure 2 Schematic of experimental set-up.

0.1 M of NaOH solution at the closing stage of each experiment. The initial pH of the solution (5.38) was slowly brought up to the minimum supersaturation limit (investigated by thermodynamic modelling) using 0.5 M and thereafter using 0.1 M of NaOH until the first appearance of instantaneous nucleation. The formation of a nuclei cloud in the solution indicated instantaneous nucleation.

In every circumstance, an approximately 15-min interval was given after each drop of NaOH addition to observe any alteration in the reactive solution. Under careful observation, the first appearance of instantaneous nucleation was detected by laser light passing through the reactive solution. Scattering of laser light was implemented parallel to the bottom and perpendicularly to the surface of the reactive solution container. Visual observation of a conditional red line was inspected perpendicularly to the laser light. To avoid any interference, laser light in the solution must not touch the impeller blade. Undersaturated solution, free from particles of significant size, did not show any distinct red-colour line of laser light since illumination of light depended on the reflection of light onto particles present in the solution. Micro-size stable struvite nuclei formed in favourable supersaturated solution. Careful observation and identification of a distinct red line in solution (in dark surroundings) ascertained the formation of a micronuclei cloud. A distinct sharp red line in the reactive supersaturated solution was visible from a few meters' distance in a dark room. Over time, stable nano-size nuclei transformed into micro-size particles when supersaturation was sufficiently high to make the nano-nuclei stable. In the absence of any diffusive body (seed crystals), unstable nuclei redissolved. The main objective of the metastable zone experiment was to identify the minimum limit of labile supersaturation at which instantaneous nucleation produced a nuclei cloud that could be precisely detected by laser light scattering.

4. Experiment on seed materials

The main purpose of this experiment was to identify the potential of different seed crystals in struvite crystallization. A series of experiments was conducted using solution at 0.002, 0.003, 0.004, 0.005, and 0.007 equi-molar concentrations of magnesium, ammonium, and phosphate. Three types of seed materials, i.e., quartz sand, borosilicate glass grindings, and previously generated struvite, were employed in the specified concentrations. Well-graded quartz sand was crushed and sieved using a 45–53-μm ASTM standard sieve followed by 24 h of oven drying at 105°C. Broken laboratory glassware was used as the source of borosilicate glass seeds following a treatment process of acid wash and drying and thereafter crushing and sieving using an ASTM standard sieve of 45–63 μm. Previously generated struvite crystals were used as mother seeds. Struvite seeds were treated by e.g. dry sieving with an ASTM standard sieve of 45–63 μm before using them as seed materials in subsequent experiments. All experiments were conducted following the schematic diagram in Figure 2 except for the application of the laser light scattering device and the darkness of the surrounding at the time of the experiment. Each solution was seeded with 1 g of the respective seed materials. All experiments were carried out at 35-rpm agitation speed along with the slow addition of NaOH solution. At the initial stage of the experi-

ment, NaOH at 0.25-M concentration was used, while close to supersaturation 0.1-M NaOH was used. All experiments were conducted within the previously investigated stable–metastable zone lying close to the minimum solubility limit.

The high-resolution pictures of the produced crystals were taken using a JOEL JSM-5410LV scanning electron microscope (SEM), which has a magnification range of 35 to 200,000. Crystal elements were analysed using the X-ray diffraction technique (XRD C). The crystal size distribution (CSD) was analysed using a Malvern particle sizer. The trend of pH change was recorded over 24 h in a data logger connected to a pH controller and a pH probe.

5. Results and discussion

The experimental pH for spontaneous precipitation was compared with the pH of minimum struvite solubility. Thermodynamic equilibria of struvite chemistry were simulated and the simulated response was verified with thermodynamic modelling developed in PHREEQC (thermodynamic modelling package) and with derived data from the Ohlinger [18] solubility limit curve. The graphical presentation of the investigated pH is shown in Figure 3. The range of maximum and minimum pH limit is documented as the operating pH range of the metastable region. Crystallization, operating along or very close to the pH of just supersaturation, can intensify crystal growth by arresting nucleation. Crystal growth in this case is governed by surface diffusion (layering) of newly born nuclei onto seed particles.

The trend of pH change during the preliminary stage of crystallization is shown in Figures 4–6. The release of H^+ in the supersaturated struvite system is an indirect approach of expressing reaction rate ensuing chemical reaction in active solution.

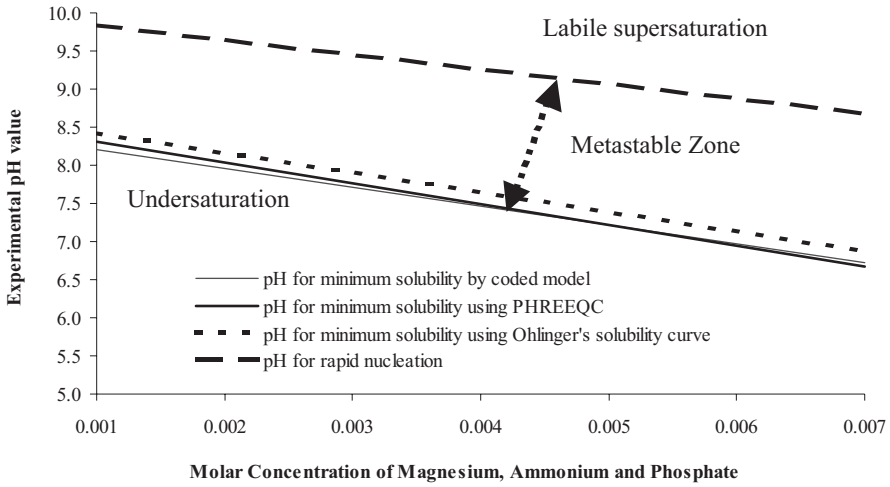

Figure 3 Identification of metastable zone for struvite crystallization.

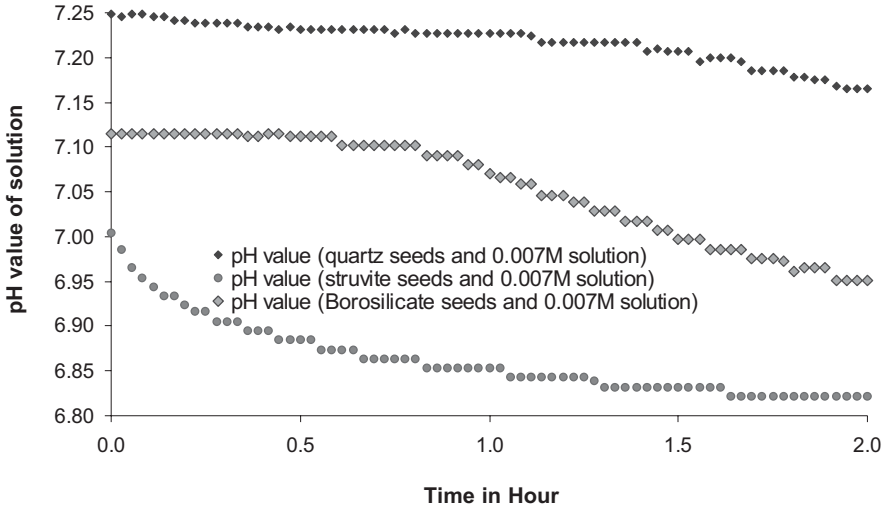

Figure 4 Reaction rate (pH drops) during experiment for 0.007-M solution.

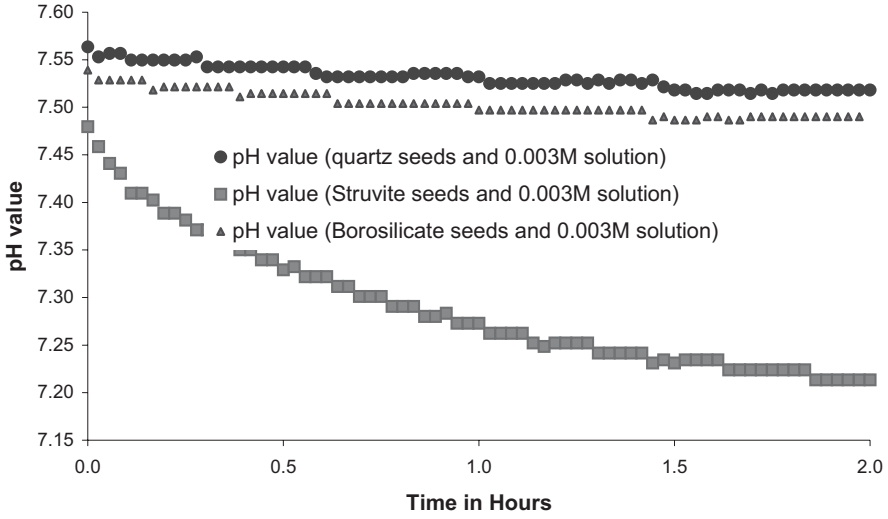

Figure 5 Reaction rate (pH drops) during experiment for 0.003-M solution.

On the basis of Eq. (12), each recordable unit of pH drop in the supersaturated struvite system represents the occurrence of reaction by means of 2 moles of H^+ release with resulting 1 mole of struvite formation when reaction takes place [17].

$$MgCl_2 + NH_4H_2PO_4 \Leftrightarrow MgNH_4PO_4 + 2H^+ \tag{12}$$

A slower reaction rate was observed for quartz sand seeds and borosilicate seeds, whereas a higher reaction rate was observed for struvite seeds due to isomorphism

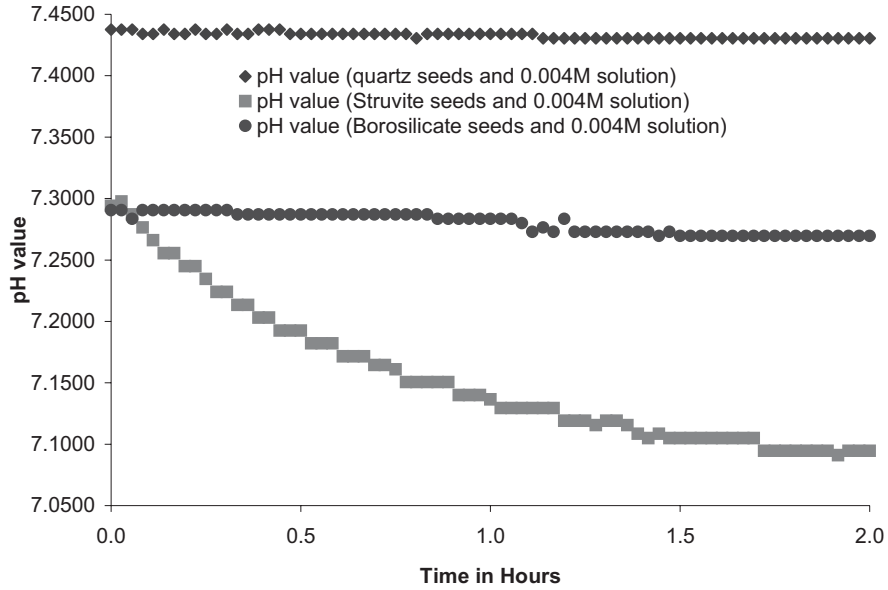

Figure 6 Reaction rate (pH drops) during experiment for 0.004-M solution.

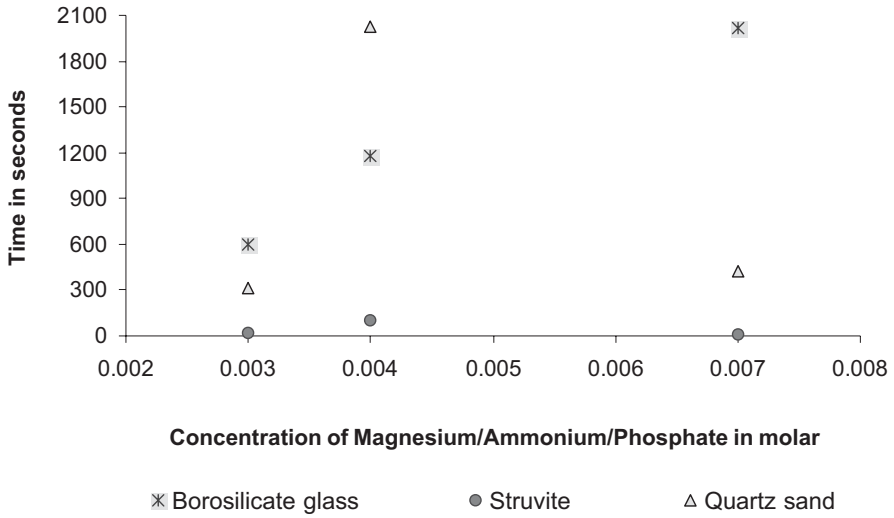

Figure 7 Experimental induction time in struvite crystallization using different seeds.

of seeds and newly born nuclei (Figures 4–6). Crystallization in the stable–metastable region (close to saturation) induced thermodynamically unstable nuclei due to very high energy consumption from the solution of very low thermodynamic driving force. The immature nuclei diffused on the isomorphous seed surface (struvite) and gained its maturation, leading to pH drops subsequent to induction lag time.

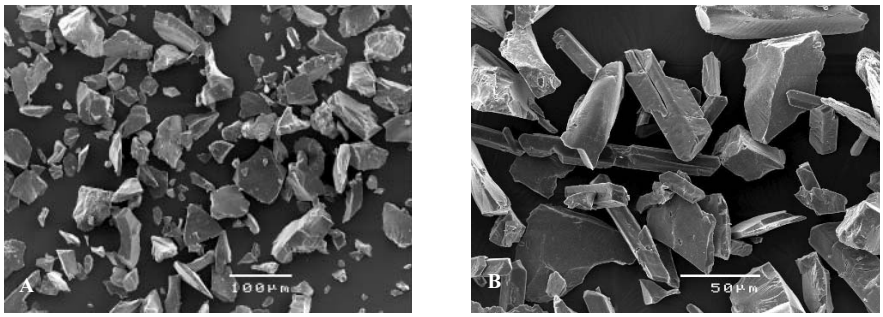

Figure 8 Scanning electron microscopic view of quartz sand seeds (A), and growing struvite with quartz sand seeds (B).

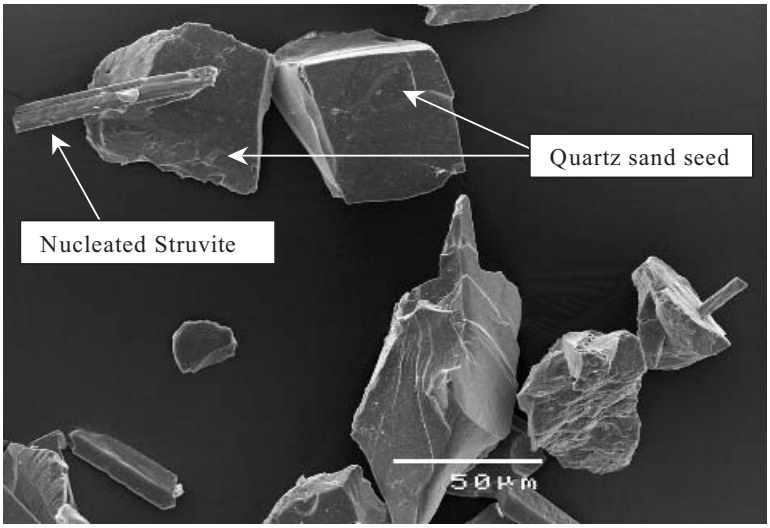

Figure 9 Magnified scanning electron microscopic view of growing struvite and quartz sand seeds.

The desupersaturation curves, represented in Figures 4–6, illustrated simultaneous nucleation, growth process of struvite crystallization with controlled and slow nucleation. The horizontal portions of each curve express a slow nucleation lag and simultaneous diffusion of the immature nuclei, afterwards a slow pulse of desupersaturation. The slower desupersaturation rate can lead to rigorous control of this system in industrial/continuous/fed-batch scale of reactor operation.

Non-isomorphous seeds acted as a diffusive body but did not take part in the integration step; therefore, unstable newly born nuclei redissolved, leading to longer or even infinite induction time (Figure 7). Therefore, it is to be concluded that isomorphous seed materials intensify crystallization when crystallization operates along the stable–metastable zone.

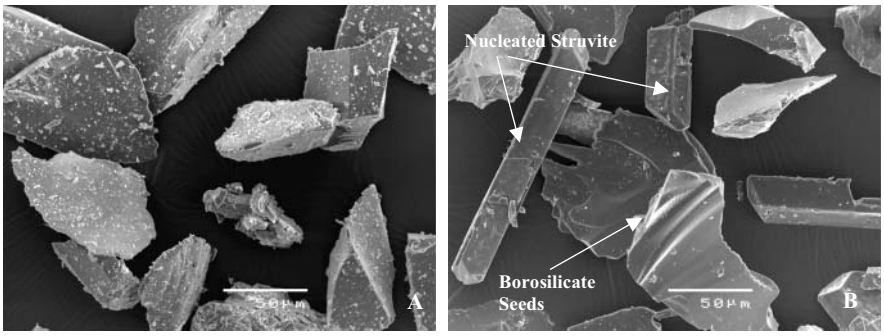

Figure 10 Scanning electron microscopic view of borosilicate seeds (A), and growing struvite along with borosilicate glass seeds (B).

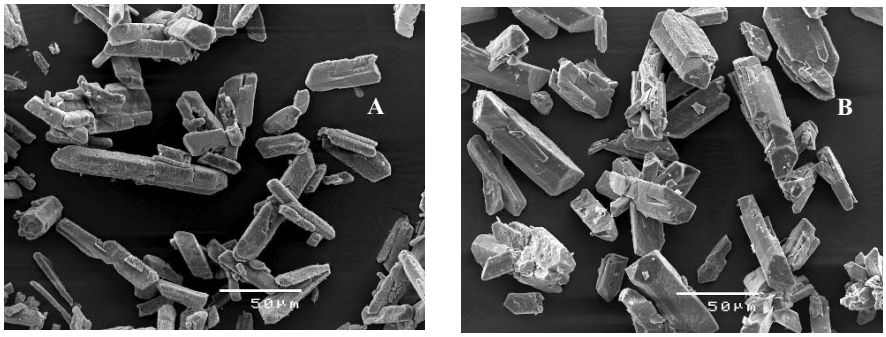

Figure 11 Scanning electron microscopic view of struvite seed (A), and growing struvite along with struvite seed (B).

Figures 8–11 show the SEM view of struvite growth using different types of seeds. Quartz seeds and borosilicate glass seeds did not take part in the growth process noticeably (Figures 8–10); however, some orthorhombic shape of struvite crystals formed due to the nucleation and subsequent to growth of stable struvite. The similarity of the lattice structure between struvite seeds and newly born struvite nuclei enhances the diffusion–integration process. However, the likelihood of the diffusion–integration process for other types of seeds is less effective due to the redissolving of unstable nuclei as explained by the Gibbs-Thompson effect of energy transformation during crystallization [1]. It is worthwhile noting that all metastable experiments were conducted very close to the saturation region, as investigated previously in thermodynamic modelling [18].

The crystal size distribution of produced struvite, using the Malvern particle sizer, is shown in Figures 12–14. Struvite growth acknowledged a size-independent growth process since the CSD curve shifted almost identically to the left. A less significant effect of agglomeration was also observed, which supplemented the per-cent volume peak. Borosilicate glass seeds and quartz sand seeds experienced less effective growth (Figure 12) than did struvite seeds (Figures 13 and 14) along with an agglomeration

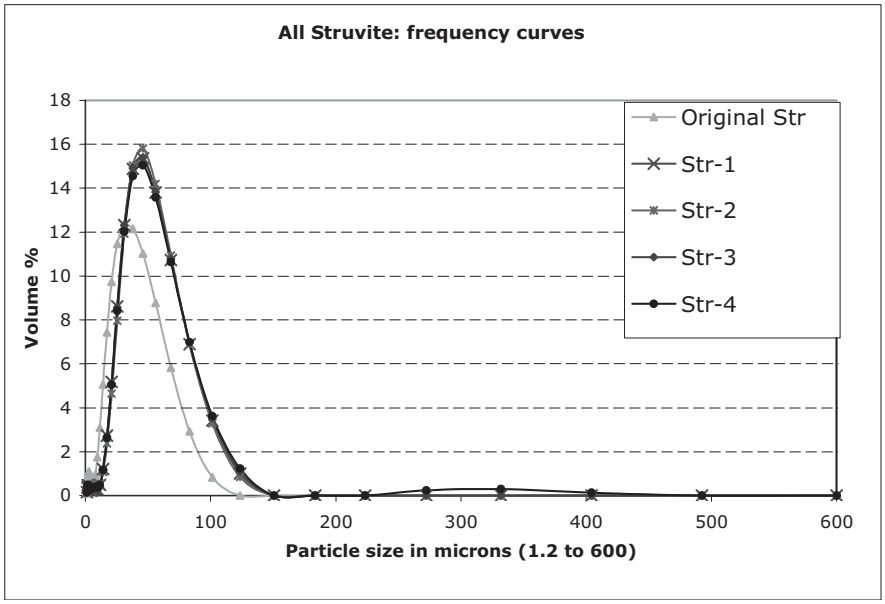

Figure 12 Crystal size distribution of struvite when struvite was used as seeds.

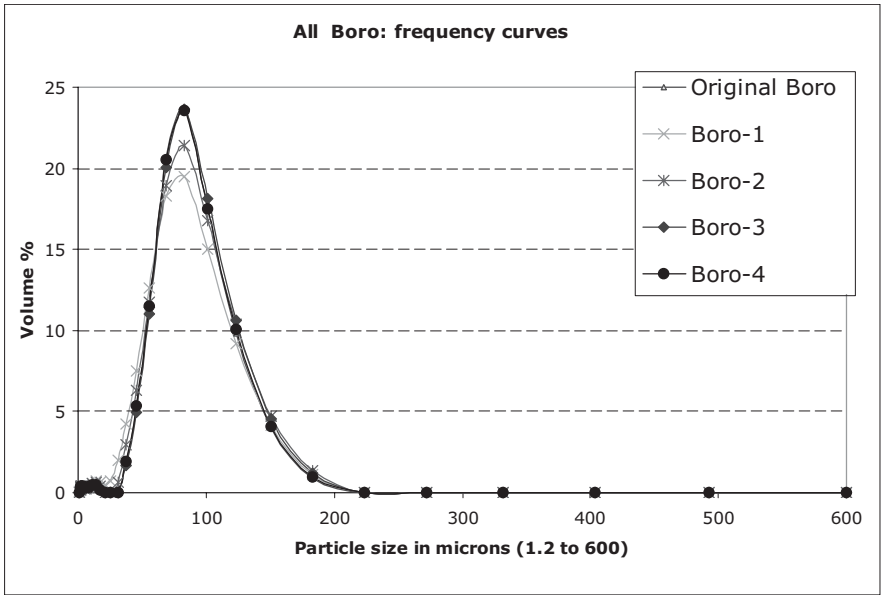

Figure 13 Crystal size distribution of struvite when borosilicate glass was used as seeds.

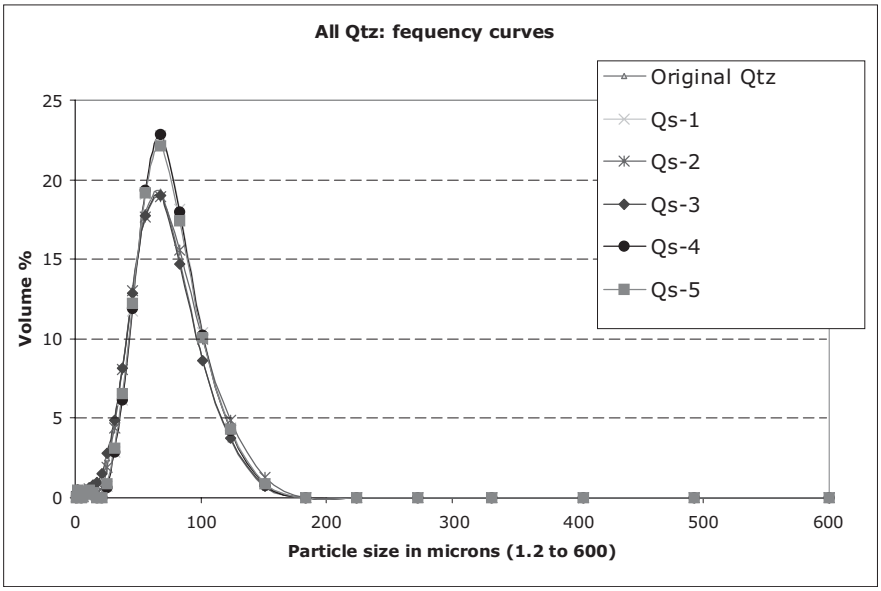

Figure 14 Crystal size distribution of struvite when quartz sand was used as seeds.

effect among the corresponding seed particles. The size-independent growth of struvite with mother seeds resulted in a diffusion–integration process of crystal growth.

Finally, the results of the batch crystallization using different types of seeds are summarized in Table 2. The results show higher growth of struvite when previously generated struvite crystals were used as seeds in the supersaturated struvite system.

Table 2 Summary of experiment of struvite crystal growth using different seed particles.

Conc. (M)	pH (S)	pH (Q)	pH (B)	SI (S)	SI (Q)	SI (B)	G (S)	OT (S)	G (Q)	OT (Q)	G (B)	OT (B)
0.003	7.48	7.637	7.54	0.06	0.11	0.08	13.44	12.29	4.96	12.57	0.53	14.67
0.004	7.294	7.564	7.29	0.02	0.32	0.02	11.81	12.14	4.42	14.67	1.99	18.51
0.007	7.004	7.245	7.116	0.22	0.51	0.36	11.44	23.64	−0.19	22.17	−3.73	19.62

6. Conclusion

The main conclusions of this paper are as follows:

1. It is possible to identify the metastable zone when the minimum struvite solubility limit and minimum limit of spontaneous nucleation are known. Laser light scattering into the reactor can detect the minimum limit of spontaneous nucleation under careful observation. The struvite solubility limit was recognized by

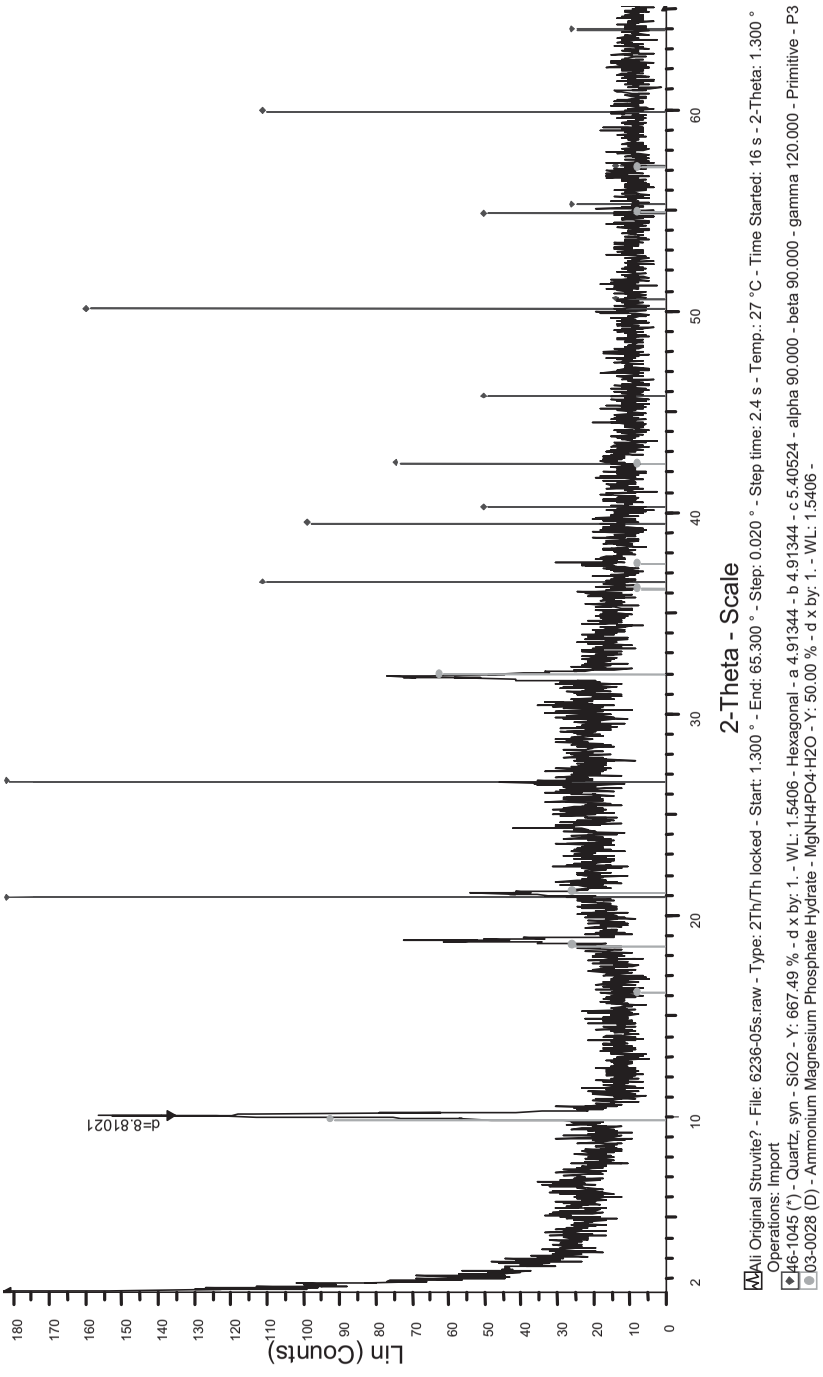

Figure 15 Analysis of struvite component and comparison with quartz using XRD.

simulating thermodynamic equilibria of struvite chemistry and was validated precisely with the PHREEQC thermodynamic modelling package and the Ohlinger [18] solubility limit curve.

2. Struvite seed proved to be more effective for struvite crystallization due to the similarity of lattice structure. The similarity of lattice structure between seed and mother crystal stimulates the diffusion–integration process of newly born crystals onto the seed surface. Therefore, mother crystals have a supportive effect on the diffusion–integration process on crystallization.
3. It is possible to crystallize struvite at very low supersaturation even along the stable–metastable zone (very close to the saturation region). Recognized size-independent growth of struvite was observed; however, an insignificant effect of agglomeration was also incurred in stable–metastable supersaturation. The produced crystal was identified as struvite by XRD analysis.

Nomenclature

Boro-1	CSD of growing struvite in 0.002-M solution along with borosilicate seeds
Boro-2	CSD of growing struvite in 0.003-M solution along with borosilicate seeds
Boro-3	CSD of growing struvite in 0.004-M solution along with borosilicate seeds
Boro-4	CSD of growing struvite in 0.007-M solution along with borosilicate seeds
Conc (M)	Molar concentration of solution
pH(S)	Initial pH value of experiment with struvite seeds
pH(Q)	Initial pH value of experiment with quartz sand seeds
pH(B)	Initial pH value of experiment with borosilicate glass seeds
Original str	Crystal size distribution (CSD) of struvite seeds in microns
OT(S)	Experimental operation time in hours with struvite seeds
OT(Q)	Experimental operation time in hours with quartz sand seeds
OT(B)	Experimental operation time in hours with borosilicate glass seeds
Qs-1	CSD of growing struvite in 0.002-M solution along with quartz sand seeds
Qs-2	CSD of growing struvite in 0.003-M solution along with borosilicate seeds
Qs-3	CSD of growing struvite in 0.004-M solution along with quartz sand seeds
Qs-4	CSD of growing struvite in 0.005-M solution along with quartz sand seeds
Qs-5	CSD of growing struvite in 0.007-M solution along with quartz sand seeds
Str-1	CSD of growing struvite in 0.002-M solution along with struvite seeds

Str-2	CSD of growing struvite in 0.003-M solution along with struvite seeds
Str-3	CSD of growing struvite in 0.004-M solution along with struvite seeds
Str-4	CSD of growing struvite in 0.007-M solution along with struvite seeds

References

[1] Mullin, J.W., Crystallization, 3rd edition, Butterworth-Heinnemann, Ipswich, UK, 1993.
[2] Myerson, A.S., Handbook of Crystallization, Butterworth-Heinnemann Series in Chemical Engineering, 1993.
[3] Munch, E.V., Barr, K., Controlled struvite crystallization for removing phosphorus from anaerobic digester side-streams, Water Res., 35 (2001), 151.
[4] Srinivasakannan, C., Vasanthakumar, R., Iyappan, K., Rao, P.G., A case study on crystallization of oxalic acid in batch cooling crystalliser, Chem. Biochem. Eng. Quarterly, 16 (2002), 125.
[5] McPherson, A., The use of heterogeneous and epitaxial nucleants to promote the growth of protein crystals, J. Cryst. Growth, 90 (1988), 47.
[6] Kim, K.J., Mersmann, A. Estimation of metastable zone width in different nucleation processes, Chem. Eng. Sci., 56 (2001), 2315.
[7] Kim, K.J., Kim, M.J., Lee, J.M., Kim, S.H., Kim, H.S., Park, B.S., Solubility, density and metastable zone width of the 3-nitro-1, 2,4-triazol-5-one + water system, J. Chem. Eng. Data, 43 (1998), 65.
[8] Scope Newsletter, 44 (2001), Original source: Hirasawa, I., Study on Recovery of Ions in Wastewater by Crystallization, Memoirs of School of Science and Engineering, Waseda University Japan, 60 (1996).
[9] Tavare, S.N., Industrial Crystallization: Process Simulation Analysis and Design, Plenum Press, New York/London, 1995.
[10] Penkova, A., Dimitrov, I., Nanev, C.N., Nucleation of insulin crystals in a wide continuous supersaturation gradient, Ann. NY Acad. Sci., 1027 (2004), 56.
[11] Webb, K.M., The solubility of struvite and its application to a piggery effluent problem, PhD Thesis, Murdoch University, School of Biological and Environmental Sciences, 1988.
[12] Paraskeva, C.A., Charalambous, P.G., Stokka, L.E., Klepetsanis, P.G., Koutsoukos, P.G., Read, P., Ostvold, T., Sand bed consolidation with mineral precipitation, J. Colloid Interface Sci., 232 (2000), 326.
[13] Nancollas, G.H., Kinetics of crystal growth from solution, J. Cryst. Growth, 3–4 (1968), 335.
[14] Joko, I., Phosphorus removal from wastewater by the crystallization method, Water Sci. Technol., 17 (1984), 121.
[15] Angel, R., Removal of phosphate from sewage as amorphous calcium phosphate, Environ. Technol., 20 (1999), 709.
[16] McCabe, W.L., Smith, J.C., Harriot, P., Unit Operation of Chemical Engineering, 4th edition, McGraw Hill Book Company, New York, 1985.
[17] Bouropoulos, C.C. and Koutsoukos, P.G., Spontaneous precipitation of struvite from aqueous solutions, J. Cryst. Growth, 213 (2000), 381.
[18] Ohlinger, K.N., Kinetics effects on preferential struvite accumulation in wastewater, PhD Thesis in School of Engineering, California State University, Davis, CA, 1999.
[19] Childs, C.W., A potentiometric study of equilibria in aqueous divalent metal orthophosphate solutions, Inorg. Chem., 9 (1970), 2465.
[20] Martell, A.E., Smith, J.C., Critical Stability Constants, Pergamon Press, New York, 1989.

[21] Morel, F.M.M., Hering, J.G., Principles and Applications of Aquatic Chemistry, John Wiley and Sons, New York, 1993.
[22] Davies, C.W., Ion Association, Butterworths, Washington, DC, 1962.
[23] Nancollas, G.H., Kinetics of crystal growth from solution, J. Cryst. Growth, 3 (1968), 335.
[24] Al-Khayat, A., Garside, J., Calcium Carbonate Precipitation: The Role and Importance of Solution Chemistry, in: 11th Symposium of Industrial Crystallization, Garmisch-Partenkirchen, 1990.

Paper received: 2004-08-10
Paper accepted: 2005-01-05